ISSN 1063-7834, Physics of the Solid State, 2022, Vol. 64, No. 2, pp. 33–37. © Pleiades Publishing, Ltd., 2022.
ISSN 1063-7834, Physics of the Solid State, 2022. © Pleiades Publishing, Ltd., 2022.
Russian Text © The Author(s), 2021, published in Fizika Tverdogo Tela, 2021, Vol. 63, No. 12, pp. 2205–2209.

Formation of the Cu_6Sn_5 Intermetallics in Cu/Sn Thin Films

L. E. Bykova[a, *], S. M. Zharkov[a, b], V. G. Myagkov[a], Yu. Yu. Balashov[a], and G. S. Patrin[a, b]

[a] *Kirensky Institute of Physics, Krasnoyarsk Scientific Center, Siberian Branch, Russian Academy of Sciences, Krasnoyarsk, 660036 Russia*

[b] *Siberian Federal University, Krasnoyarsk, 660041 Russia*

**e-mail: lebyk@iph.krasn.ru*

Received July 25, 2021; revised July 25, 2021; accepted August 4, 2021

Abstract—The formation of the Cu_6Sn_5 intermetallic in Sn(55nm)/Cu(30nm) thin-film bilayers has been studied upon heating the film sample from room temperature to 300°C directly in a column of a transmission electron microscope in the electron diffraction mode with recording electron diffraction patterns. The thin films synthesized by the solid-state reaction have been found to be single-phase and consist of the η-Cu_6Sn_5 hexagonal phase (95–260°C). It has been suggested basing on the effective interdiffusion coefficient (5×10^{-16} m^2/s) estimated in the course of the reaction that the main mechanism of the formation of the Cu_6Sn_5 thin films is diffusion along grain boundaries and dislocations.

Keywords: thin films, Cu_6Sn_5 intermetallic, transmission electron microscopy, electron diffraction

DOI: 10.1134/S1063783422010048

1. INTRODUCTION

The benefits of Cu–Sn alloy-based lead-free solders for the environment and human health have prompted investigations of the properties and behavior of the Cu–Sn system [1]. The reaction between Cu and Sn that occur during soldering electronic devices with Cu–Sn solders causes the intense formation of a Cu_6Sn_5 intermetallic [2–4]. As the devices become increasingly miniature, the fraction of the intermetallic layer in the total thickness of a solder joint grows. The Cu_6Sn_5 intermetallic compound is an important material for production of lithium battery anodes [5, 6].

As is known, the phase transformations in the Cu_6Sn_5 intermetallic significantly affect the reliability of electronic devices. Therefore, the knowledge of the crystal structure of the Cu_6Sn_5 intermetallic and phase transformations in it is required to understand changes in its properties during soldering and operation of electronic devices. The Sn/Cu binary thin films are convenient objects for studying structural changes that occur during the production and use of the Cu_6Sn_5 intermetallic.

To date, the crystal structures of several Cu_6Sn_5 modifications have been studied and identified. The differences in the crystal structure result from changes in the composition and depend on a processing technique used [7–10]. According to the Cu–Sn phase diagram [11], the Cu_6Sn_5 (54.5 at % Cu) compound in the solid state has two crystal structures. The monoclinic η'-Cu_6Sn_5 structure (sp. gr. *C*2/*c*) is stable at temperatures below 186°C, while the hexagonal η-Cu_6Sn_5 structure (sp. gr. $P6_3/mmc$) is stable above this temperature. As the temperature decreases below 186°C, the polymorphic phase transformation $\eta \rightarrow \eta'$ occurs. According to the room-temperature density data, the polymorphic transformation $\eta \rightarrow \eta'$ in the Cu_6Sn_5 compound leads to a volume expansion by 2.15% [10], which induces undesirable internal stresses in the intermetallic layer.

This work presents the results of the synthesis of the Cu_6Sn_5 intermetallic thin films carried out directly in a column of a transmission electron microscope (TEM) by heating a Sn/Cu bilayer sample from room temperature to 300°C in the electron diffraction mode. The main synthesis parameters and a change in the phase composition during the solid-phase reaction between the Cu and Sn layers are determined.

2. EXPERIMENTAL

In the synthesis of the Sn(55 nm)/Cu(30 nm) bilayer films, the Cu and Sn layer thicknesses were chosen according to the ratio of the Cu_6Sn_5 intermetallic composition (~54.5 at % of Cu and ~45.5 at % of Sn).

The synthesis of initial Sn/Cu bilayers included successive thermal deposition of the Cu and Sn films with respective thicknesses of ~30 and ~55 nm in vacuum at a residual pressure of 1.3×10^{-4} Pa. The Cu layer was deposited onto a freshly cleaved NaCl(001)

single crystal heated to a temperature of 200°C to ensure the Cu(111) epitaxial growth relative to the substrate surface. To prevent an uncontrolled reaction between the Sn and Cu layers, a ~55-nm-thick Sn layer was deposited on top of the Cu layer at room temperature. For the evaporation, the high-purity materials were used: Cu (99.99%) and Sn (99.995%). The Sn and Cu layer thicknesses were determined by X-ray fluorescence analysis; the total Sn/Cu film thickness was ~85 nm.

To carry out the TEM investigations, the synthesized Sn/Cu/NaCl(001) films were separated from the NaCl(001) substrate in distilled water at room temperature, deposited onto molybdenum supporting grids for the TEM study, and placed on a heater in an electron microscope. The film sample was heated directly in a column of a transmission electron microscope using a special Gatan Model 652 double tilt heating holder, which allows one to control heating of a sample from room temperature to 1000°C. The samples were heated from room temperature to 300°C at a rate of 4°C/min with recording electron diffraction patterns in an interval of 1°C. The analysis of the electron diffraction patterns yielded data on a change in the phase composition of the samples upon heating.

The structure and local elemental composition of the obtained samples were studied on a JEOL JEM-2100 transmission electron microscope equipped with an Oxford Inca X-sight energy dispersive spectrometer at an accelerating voltage of 200 kV. The intensities of reflections in electron diffraction patterns were analyzed and interpreted using the Gatan Digital Micrograph software and the ICDD PDF 4+ database [12].

3. RESULTS AND DISCUSSION

The initial Sn/Cu samples were bilayers consisting of Sn and Cu nanolayers. The electron diffraction pattern of the initial Sn/Cu film (Fig. 1) contains the diffraction reflections characteristic of the β-Sn phase (sp. gr. $I4_1/amd$; the lattice parameters are $a = 5.831$ Å, $b = 5.831$ Å, and $c = 3.182$ Å; PDF card no. 00-004-0673) and the Cu phase (sp. gr. $Fm3m$; the lattice constant is $a = 3.615$ Å; PDF card no. 00-004-0836). Copper deposited onto the NaCl(001) substrate had the [111] preferred crystallographic orientation relative to the substrate plane. No reflections from Sn_xCu_{1-x} intermetallics were observed.

The sample was heated from room temperature to 300°C at a rate of 4°C/min in an electron microscope column in the electron diffraction mode. The diffraction pattern remained unchanged until the temperature attained 95°C, when, in addition to the reflections corresponding to the Cu and β-Sn phases, the diffraction reflections from the η-Cu_6Sn_5 phase (sp. gr. $P6_3/mmc$; the lattice parameters are $a = 4.206$ Å and $c = 5.097$ Å; PDF card no. 00-047-1575) appeared, which indicated the beginning of the reac-

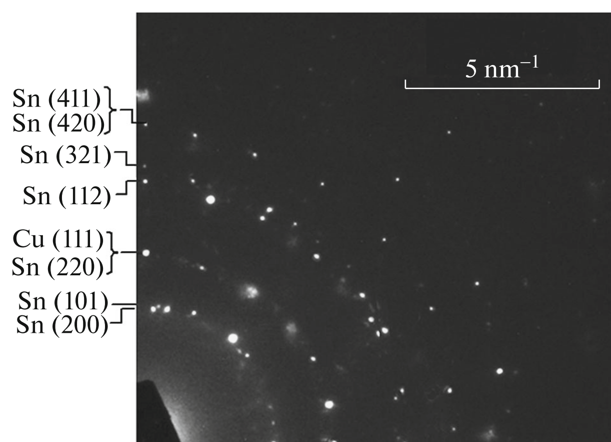

Fig. 1. Electron diffraction pattern of the initial Sn/Cu film.

tion between the Cu and Sn nanolayers. Figures 2a and 2b show electron diffraction patterns obtained at 100 and 200°C, respectively, which contain the reflections corresponding to the η-Cu_6Sn_5 phase; the intensity of the reflections corresponding to the Cu and Sn phases decreases with increasing temperature; i.e., the reaction between Cu and Sn continues. When the heating temperature exceeded the Sn melting point ($T_m = 231.9$°C), the reflections corresponding to the Sn phase disappeared from the electron diffraction pattern (Fig. 3a). Upon heating from 260 to 300°C (Fig. 3a) and after cooling the sample to 25°C (Fig. 3b), only the reflections from the hexagonal η-Cu_6Sn_5 phase were observed, which confirmed that Cu and Sn have completely reacted. Upon cooling the film from 300 to 25°C, no phase transformation $\eta \rightarrow \eta'$ was observed.

The diffraction reflections corresponding to the η'-Cu_6Sn_5 phase (sp. gr. $C2/c$; the lattice parameters are $a = 10.926$ Å, $b = 7.113$ Å, and $c = 9.674$ Å; PDF card no. 04-014-9975) appeared in the electron diffraction pattern after aging the film for one month at room temperature (Fig. 4). This points out the occurrence of the polymorphic phase transformation $\eta \rightarrow \eta'$ and the film represents a mixture of the η and η' phases.

It follows from the foregoing that the Cu_6Sn_5 intermetallic was formed in the temperature range of 95–260°C, which corresponds to a reaction time of $t \approx 2.5 \times 10^3$ s and a heating rate of 4°C/min. Assuming a weak temperature dependence of diffusion in the temperature range of 95–260°C and estimating the reaction diffusion using the equation $d^2 = 6D_{\text{eff}}t$, we can determine the order of the effective diffusion coefficient $D_{\text{eff}} \approx 5 \times 10^{-16}$ m^2/s, where $d = 85$ nm is the total film thickness. The calculated diffusion coefficient is relatively high. The experimental diffusion coefficients for most metals in the thin films range

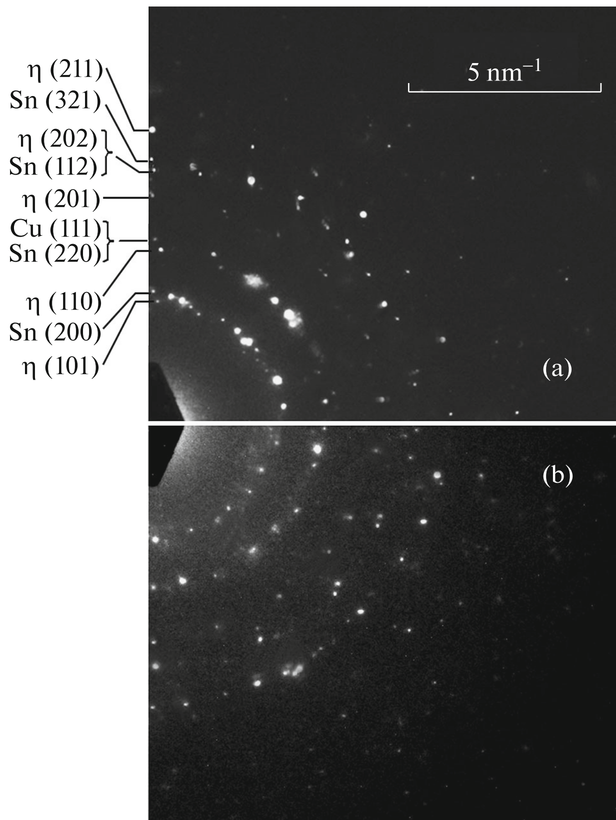

Fig. 2. Electron diffraction patterns of the Sn/Cu film after heating at temperatures of (a) 100°C and (b) 200°C.

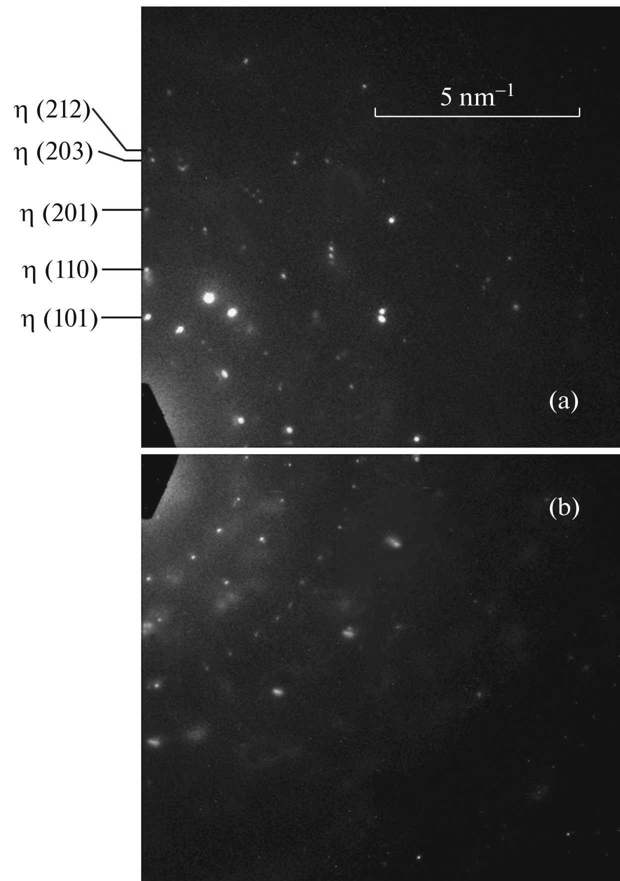

Fig. 3. Electron diffraction patterns of the Sn/Cu film after (a) heating at a temperature of 300°C and (b) cooling to 25°C.

within 10^{-22}–10^{-16} m^2/s at 100–800°C [13]. It can be assumed that diffusion along dislocations and grain boundaries is the main mechanism that determines the formation of the Cu_6Sn_5 intermetallic in the course of the solid-state reaction between the Sn and Cu nanolayers.

The TEM image of the film (Fig. 5) shows the developed growth of η-Cu_6Sn_5 during the solid-state reaction. An increase in the sample temperature from 100 to 300°C led to a significant coarsening (over 100 nm) of Cu_6Sn_5 grains (Figs. 5b–5d). The grain growth continued upon cooling the film from 300 to 25°C (Fig. 5e). After aging the film for one month at room temperature, the TEM image of the film (Fig. 5f) showed a decrease in the η-Cu_6Sn_5 grain size due to the phase transformation η → η'.

Thus, it was shown that the η-Cu_6Sn_5 phase forms at an initiation temperature of $T_{in} \approx 95$°C and passes to the η'-Cu_6Sn_5 phase after aging the film at room temperature for one month. The results obtained are consistent with the data of Zhong et al. [14], who studied the formation of nanocrystalline Cu_6Sn_5 alloys through the polymorphic reversible phase transformation η ↔ η', and with the data of Zhang et al. [15], who reported the phase transformation η-Cu_6Sn_5 → η'-Cu_6Sn_5 in whiskers during the room-temperature aging for 1–40 days.

Previously (see [16] and references therein), we showed that, with an increase in the annealing tem-

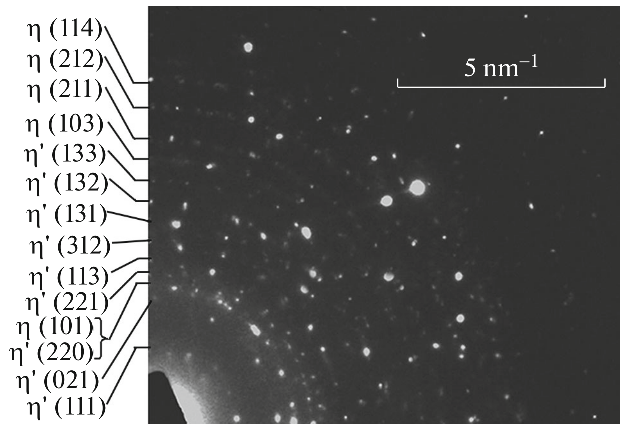

Fig. 4. Electron diffraction pattern of the Cu_6Sn_5 film after exposure for one month at room temperature.

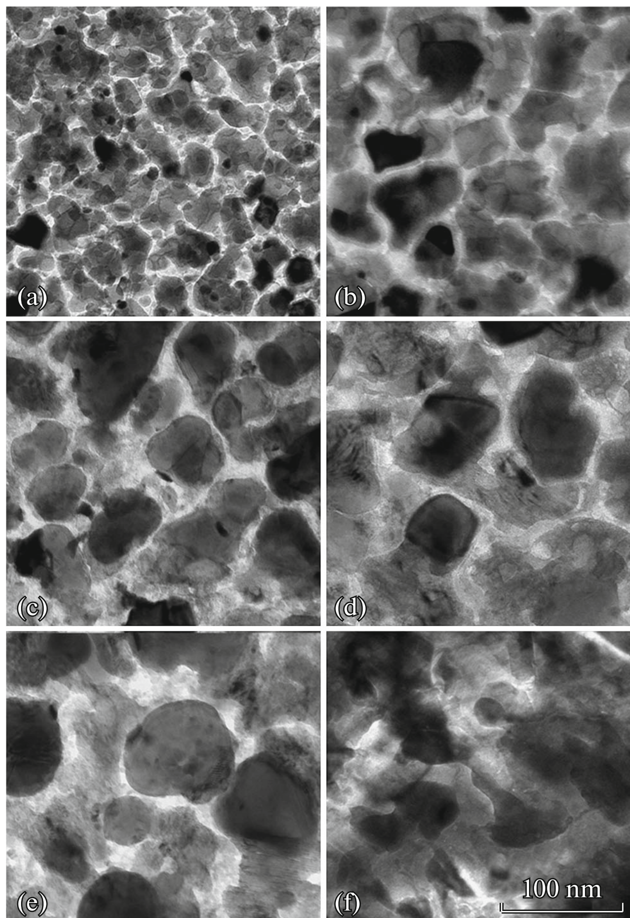

Fig. 5. Transmission electron microscopy images of the surface of the Sn/Cu film (a) in the initial state; after heating at (b) 100, (c) 200, and (d) 300°C; (e) after cooling from 300 to 25°C; and (f) after aging the obtained Cu_6Sn_5 film for one month at room temperature.

perature at the interface between films, one phase forms among many phases observed in the phase diagram of a binary system, which is called the first phase and has the minimum temperature of the structural solid-state transformation in this binary system. Next, with an increase in the annealing temperature, other phases can emerge with the formation of a phase sequence. In the Cu–Sn system, the structural transition $\eta \rightarrow \eta'$ has a minimum temperature in the phase diagram; therefore, we can conclude that, in all cases, with an increase in temperature at the copper/tin interface, the Cu_6Sn_5 intermetallic forms first. This is confirmed by the present study and analysis of studies on the phase formation at the Cu/Sn interface by other authors [3, 10].

4. CONCLUSIONS

The Cu_6Sn_5 intermetallic in the Sn(55 nm)/Cu(30 nm) thin films was formed by heating directly in a column of a transmission electron microscope in the electron diffraction mode from room temperature to 300°C. The thicknesses of the Cu and Sn layers is chosen so as to correspond to the Cu_6Sn_5 composition ratio (~54.5 at % of Cu and ~45.5 at % of Sn). The η-Cu_6Sn_5 phase starts forming at an initiation temperature of $T_{in} \approx 95$°C; at 260°C, the solid-state reaction proceeds over the entire film thickness of d = 85 nm. Upon cooling the film in an electron microscope column from 300 to 25°C, the phase transformation η-$Cu_6Sn_5 \rightarrow \eta'$-$Cu_6Sn_5$ was not observed. The effective interdiffusion coefficient ($D_{eff} \approx 5 \times 10^{-16}$ m^2/s) estimated in the course of a solid-state reaction between the Cu and Sn nanolayers suggests that the main mechanism for the formation of the Cu_6Sn_5 intermetallic is diffusion along grain boundaries and dislocations. After holding the film at room temperature for one month, the hexagonal η-Cu_6Sn_5 phase partially passed into the monoclinic η'-Cu_6Sn_5 phase, which led to the volumetric expansion, internal stresses, and a decrease in the Cu_6Sn_5 grain size.

ACKNOWLEDGMENTS

The authors thank V.S. Zhigalov for preparing the samples for investigations.

FUNDING

The study was supported by the Russian Foundation for Basic Research, project no. 19-43-240003. The electron microscopy study was carried out at the Krasnoyarsk Regional Center for Collective Use of the Krasnoyarsk Scientific Center, Siberian Branch of the Russian Academy of Sciences and at the Laboratory of Electron Microscopy of the Center for Collective Use of the Siberian Federal University within the state assignment of the Ministry of Science and Higher Education of the Russian Federation, research theme code FSRZ-2020-0011.

CONFLICT OF INTERESTS

The authors declare that they have no conflicts of interest.

REFERENCES

1. S. Cheng, C. M. Huang, and M. Pecht, Microelectron. Reliab. **75**, 77 (2017). https://doi.org/10.1016/j.microrel.2017.06.016
2. A. Kunwar, J. Hektor, S. Nomoto, Yu. A. Coutinho, and N. Moelans, Int. J. Mech. Sci. **184**, 105843 (2020). https://doi.org/10.1016/j.ijmecsci.2020.105843
3. F. Somidin, H. Maeno, M. A. A. Mohd Salleh, X. Q. Trana, S. D. McDonalda, S. Matsumura, and K. Nogita, Mater. Charact. **138**, 113 (2018). https://doi.org/10.1016/j.matchar.2018.02.006
4. L. Meinshausen, H. Frémont, K. Weide-Zaage, and B. Plano, Microelectron. Reliab. **53**, 1575 (2013). https://doi.org/10.1016/j.microrel.2013.07.038

5. R. Z. Hu, M. Q. Zeng, and M. Zhu, Electrochim. Acta **54**, 2843 (2009).
https://doi.org/10.1016/j.electacta.2008.11.021
6. Ya. Xing, S. Wang, B. Fang, Y. Feng, and S. Zhang, Microporous Mesoporous Mater. **261**, 237 (2018).
https://doi.org/10.1016/j.micromeso.2016.11.036
7. G. Zeng, S. D. McDonald, J. J. Read, Q. Gu, and K. Nogita, Acta Mater. **69**, 135 (2014).
https://doi.org/10.1016/j.Actamat.2014.01.027
8. Y. Q. Wu, J. C. Barry, T. Yamamoto, Q. F. Gu, S. D. McDonald, S. Matsumura, H. Huang, and K. Nogita, Acta Mater. **60**, 6581 (2012).
https://doi.org/10.1016/j.Actamat.2012.08.024
9. D. K. Mu, S. D. McDonald, J. Read, H. Huang, and K. Nogita, Solid State Mater. Sci. **20**, 55 (2016).
https://doi.org/10.1016/j.cossms.2015.08.001
10. M. Y. Li, Z. H. Zhang, and J. M. Kim, Appl. Phys. Lett. **98**, 201901 (2011).
https://doi.org/10.1063/1.3590715
11. N. Saunders and A. P. Miodownik, Bull. Alloys Phase Diagr. **11**, 278 (1990).
12. Powder Diffraction File (PDF 4+, 2018), Inorganic Phases Database (Int. Center Diffract. Data (ICDD), Swarthmore, PA, USA, 2018).
http://www.icdd.com/products/pdf4.htm.
13. A. Makovec, G. Erdélyi, and D. L. Beke, Thin Solid Films **520**, 2362 (2012).
https://doi.org/10.1016/j.tsf.2011.11.013
14. Y. Zhong, C. Wang, J. Wang, H. Ma, S. Krishnamoorthy, V. Paley, Z. Weng, and S. Jin, Mater. Res. Lett. **8**, 431 (2020).
https://doi.org/10.1080/21663831.2020.1791272
15. Z. H. Zhang, C. W. Wei, J. J. Han, H. J. Cao, H. T. Chen, and M. Y. Li, Acta Mater. **183**, 340 (2020).
https://doi.org/10.1016/j.Actamat.2019.11.032
16. V. G. Myagkov, L. E. Bykova, V. S. Zhigalov, A. A. Matsynin, D. A. Velikanov, and G. N. Bondarenko, J. Alloys Compd. **861**, 157938 (2021).
https://doi.org/10.1016/j.jallcom.2020.157938

Translated by E. Bondareva